1986

Simple Models for Diaphragm-Type Chlorine/Caustic Cells I. Dynamic Behavior

John Van Zee
University of South Carolina - Columbia, vanzee@engr.sc.edu

Ralph E. White
University of South Carolina - Columbia, white@cec.sc.edu

A T. Watson
Texas A & M University - College Station

Publication Info

Journal of the Electrochemical Society, 1986, pages 501-507.

Publisher's Version: http://dx.doi.org/10.1149/1.2108609
DOI: 10.1149/1.2108609

Simple Models for Diaphragm-Type Chlorine/Caustic Cells

I. Dynamic Behavior

John Van Zee*

Department of Chemical Engineering, University of South Carolina, Columbia, South Carolina 29208

R. E. White* and A. T. Watson

Department of Chemical Engineering, Texas A&M University, College Station, Texas 77843

ABSTRACT

A simple model of the dynamic behavior of a diaphragm-type chlorine/caustic cell is presented. The model is based upon measurable diaphragm properties and the mass transfer of hydroxyl ion through the diaphragm. The anolyte is modeled simply as a region in which the OH^- ion concentration is fixed, the diaphragm is modeled as a plug-flow reactor with an electrochemical reaction occurring at the catholyte/diaphragm interface where the cathode is placed, and the catholyte is modeled as a completely stirred flow reactor. Analytical integration of the governing equations for these models yields two mathematical expressions: one for the concentration distribution of hydroxyl ion within the diaphragm and one for the effluent concentration. Both of these expressions are functions of time, independent operating variables, diaphragm properties, and physical constants. They are used to show how the concentration distribution of OH^- within the diaphragm and the cell effluent change when subjected to a step change in the current density. Also presented is a numerical method of solution for the model equations to predict the required change of the cell head subject to an arbitrary time-dependent change in the current density at a fixed cell effluent concentration.

Diaphragm-type cells are used extensively in the United States to produce chlorine and caustic (1). The diaphragm is the key to efficient cell operation, because the diaphragm properties affect the voltage loss, the yield, and the effluent caustic concentration. Recently (2, 3, 4), measurable diaphragm properties have been proposed and used to predict the performance of these cells under steady-state conditions. A simple model[1] of the cell is presented here to predict the effect of these diaphragm properties on the dynamic behavior of the caustic yield.

The time-dependent or dynamic behavior of diaphragm-type cells is of interest during start-up and in situations where a differential cost structure for electricity provides an opportunity to reduce the cost of production by operating the cells accordingly. This may mean a high production rate during the night and a low production rate during the day, for example. The model presented in this paper can be used to predict the changes in the operating conditions (*e.g.*, current density and differential head) which would be required to maintain a fixed caustic effluent concentration or a fixed caustic yield.

In a diaphragm-type chlorine/caustic cell (see Fig. 1), hydroxyl ions are produced at the cathode according to the following electrochemical reaction

$$H_2O + e^- \rightarrow OH^- + 1/2\ H_2 \qquad [1]$$

The buoyancy of the hydrogen gas causes stirring in the catholyte and this compartment is consequently assumed to be completely mixed. A similar statement could be made concerning the anolyte and the chlorine gas generated at the anode. This is, however, not necessary here since the anolyte is modeled simply as a region in which the OH^- ion concentration is fixed at a known value that depends on the fixed anolyte *p*H. As shown in Fig. 1, a differential head forces anolyte to percolate through the diaphragm from the anolyte to the catholyte. This percolation rate decreases the loss of OH^- ions from the catholyte to the anolyte due to diffusion and migration. However, this percolation rate should not be too large because the catholyte OH^- concentration decreases as the percolation rate increases which leads to a larger steam requirement if the cell effluent is to be concentrated to 50 weight percent NaOH. Increasing the current density increases the OH^- ion concentration in the catholyte but also increases the voltage drop through the diaphragm and hence increases the loss of OH^- ions due to migration. Also, the diaphragm characteristics affect the loss of OH^- ions due to diffusion, migration, and percolation velocity. The time-dependent behavior of the caustic yield depends upon these losses of OH^- ions from the catholyte, the volume of the catholyte, and other operating variables and parameters, as discussed below.

Literature

In a recently reported experiment (2), two measurable quantities were used to characterize the diaphragm in a metal-anode Cl_2/NaOH electrolyzer when the velocity was specified (3, 4). These two properties are the MacMullin number, N_M, and the diaphragm thickness, L. The MacMullin number is defined (2-6) in terms of readily measurable quantities and can be thought of as the ratio of the diaphragm tortuosity and porosity

$$N_M = \frac{\rho_*}{\rho_0} = \frac{\tau}{\epsilon} \qquad [2]$$

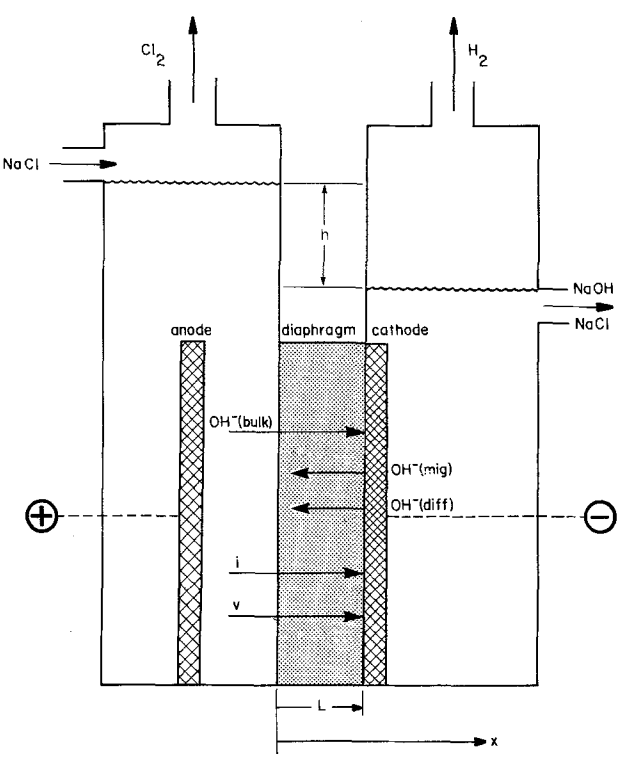

Fig. 1. A schematic of a diaphragm-type chlorine/caustic cell

*Electrochemical Society Active Member.

[1]The phrase "simple model" is used here to mean a model with a linear potential gradient through the diaphragm.

The ratio ρ/ρ_o represents the resistivity of an electrolyte-saturated porous medium to that of the pure electrolyte. This ratio denoted here as N_M, has been referred to by others as the formation factor (7) and the labyrinth factor (8). Other diaphragm properties have also been proposed (9-15), but none of these is measurable directly, even though they have been shown to be equivalent to the product $N_M L$ (3, 4, 16).

Simple steady-state models of the diaphragm-type cell for chlor-alkali cells have been presented and reviewed recently (3, 4). More complete models have also been presented (5, 17). One of these models (5) was used to analyze steady-state phenomena, including the assumption of a reaction plane for dissolved chlorine species in the diaphragm; however, only the essence of the model was presented for proprietary reasons. The other model (17) used numerical integration to analyze the distribution of Na^+, Cl^-, and OH^-, and a nonlinear potential gradient in the diaphragm, but diaphragm properties were not included in the model.

Time-dependent models of a diaphragm-type electrolyzer have also been presented (17-22). Some of these models (18-20) are based on an empirical expression for the caustic yield, whereas Filatov *et al.* (21) based their model on the assumption that the anolyte and catholyte are completely stirred flow reactors (CSFR). They connected the CSFR material balances for the anolyte and catholyte with an analytical steady-state expression for the diaphragm/catholyte concentration that does not include diaphragm properties. Other models (22, 17) include simultaneously the catholyte chamber and the diaphragm but, again, neglect diaphragm properties. These investigators (22, 17) used numerical integration of the time-dependent, dilute solution convective diffusion equations for their models. Unfortunately, the results were limited for one of the models (22) because the numerical integration did not converge for steep gradients in the concentration. In the other model, the concentrations of Na^+, Cl^-, and OH^- were included together with a nonlinear potential gradient through the diaphragm. However, again the authors (17) did not include diaphragm properties in their work but instead claim that the diaphragms used in their comparison with data were very inhomogeneous.

Model

The model will be presented by first reviewing the time-dependent material balance equation and the flux equation for species i in a porous medium followed by presenting the assumptions of the model and the development of the equations.

A time-dependent material balance equation for a charged species within a porous region has been formulated in terms of average quantities (23-25). For the case of no electrochemical or homogeneous reactions, the material balance equation for species i can be written (24) as follows

$$\frac{\partial(\epsilon c_i)}{\partial t} = -\underline{\nabla} \cdot \underline{N}_i \qquad [3]$$

where

$$\frac{\underline{N}_i}{\epsilon} = -(D_{i,o} + D_a)\,\underline{\nabla} c_i - z_i u_i \mathbf{F} c_i \underline{\nabla}\Phi + \frac{\underline{v}\, c_i}{\epsilon} \qquad [4]$$

In Eq. [4], $\underline{v}$ is the superficial velocity (*i.e.*, the volumetric flow rate entering the diaphragm divided by the projected diaphragm area, A_d) and $\underline{v}/\epsilon$ is the velocity in the pores. Also, according to Newman and Tiedemann (24), the ionic diffusion coefficient, $D_{i,o}$, the axial dispersion coefficient, D_a, and the ionic mobility u_i in Eq. [4] are all corrected for the tortuosity of the pores, τ, but not for the porosity, ϵ.

The assumptions of the model presented here are: (*i*) only the OH^- ion is important, and it exists only in the diaphragm and catholyte; (*ii*) dilute solution theory (26) applies, and the cell is isothermal; (*iii*) only the spatial coordinate through the diaphragm in the direction of flow is important; (*iv*) the diaphragm porosity, MacMullin number, permeability, and thickness are constant with time; (*v*) the dispersion coefficient, D_a, is negligible and the effective diffusion coefficients in the porous diaphragm can be written in terms of the measurable property N_M as follows

$$D_{i,e} = \epsilon D_{i,o} = D_i/(\tau/\epsilon) = D_i/N_M \qquad [5]$$

(*vi*) the current density through the diaphragm is simply related to the potential gradient through the diaphragm by an effective average specific conductivity (3) as follows

$$i = \frac{-\kappa}{N_M}\frac{d\Phi}{dx} \qquad [6]$$

(*vii*) the percolation velocity through the diaphragm is related to the differential head, h, according to Darcy's law, with an average viscosity for the solution within the diaphragm and a pressure drop through the diaphragm given by $\rho g h$ where ρ is the density of the anolyte as follows (16)

$$v = \frac{P}{\mu}\frac{\rho g h}{L} \qquad [7]$$

(*viii*) water vapor loss from the anolyte and catholyte is negligible, so that the velocity of the feed to the cell and the velocity of the effluent are equal; (*ix*) the gas generation provides sufficient mixing so that the catholyte is a completely mixed flow reactor; (*x*) hydroxyl ions do not participate in any homogeneous reactions.

With these assumptions, the unsteady-state material balance for the hydroxyl ion ($i = 1$) in the diaphragm (Eq. [3]) for one spatial coordinate can be written

$$\epsilon\frac{\partial c_1}{\partial t} = -\frac{\partial N_1}{\partial x} \qquad [8]$$

The flux expression for Eq. [8] can be obtained from Eq. [4] by using the Nernst-Einstein expression for the ionic mobility (26), so that Eq. [4] becomes

$$\frac{N_1}{\epsilon} = -D_{1,o} + D_a\frac{\partial c_1}{\partial x} - \frac{z_1 \mathbf{F} D_{1,o} c_1}{RT}\frac{\partial\phi}{\partial x} + \frac{v c_1}{\epsilon} \qquad [9]$$

which, with assumptions (*v*)-(*vii*), becomes

$$N_1 = -\frac{D_1}{N_M}\frac{\partial c_1}{\partial x} + \left(\frac{z_1 \mathbf{F} D_1 i}{RT\kappa} + \frac{P\rho g h}{\mu L}\right) c_1 \qquad [10]$$

Thus, the governing partial differential equation for the hydroxyl ion concentration within the diaphragm can be written as

$$\frac{\partial c_1}{\partial t} = \frac{D_1}{N_M\epsilon}\frac{\partial^2 c_1}{\partial x^2} - \left(\frac{z_1 \mathbf{F} D_1 i}{RT\kappa\epsilon} + \frac{P\rho g h}{\mu L\epsilon}\right)\frac{\partial c_1}{\partial x} \qquad [11]$$

An appropriate set of initial and boundary conditions is

$$\text{at } t = 0 \qquad c_1(x, t) = c_1(x, 0) = c_1^*(x) \qquad [12]$$

$$\text{for } t > 0 \text{ at } x = 0 \qquad c_1(x, t) = c_1(0, t) = E \qquad [13]$$

$$\text{for } t > 0 \text{ at } x = L \qquad N_1(L, t) = \frac{P\rho g h}{\mu L} c_1(L, t) - \frac{i}{\mathbf{F}} \qquad [14]$$

where E is equal to the square root of the inverse of the equilibrium constant for the reaction between H^+ and OH^-, which is assumed to occur at the anolyte face of the diaphragm and where $N_1(L, t)$ is given by Eq. [10], evaluated at $x = L$.

Equations [11]-[14] can be simplified by defining the following dimensionless variables

$$\xi = \frac{x}{L} \quad [15]$$

and

$$\Theta_1(\xi, t) = \frac{c_1(x, t)}{c_F} \quad [16]$$

where c_F is the concentration of NaCl in the brine feed to the cell. Substitution of Eq. [15] and [16] into Eq. [11] yields

$$\gamma \frac{\partial \Theta_1}{\partial t} = \frac{\partial^2 \Theta_1}{\partial \xi^2} - A_1 \frac{\partial \Theta_1}{\partial \xi} \quad [17]$$

where

$$\gamma = \frac{\epsilon N_M L^2}{D_1} \quad [18]$$

and

$$A_1 = \frac{-\mathbf{F} i N_M L}{RT\kappa} + \frac{\rho g h\, PN_M}{\mu D_1} \quad [19]$$

Also, substitution of Eq. [15] and [16] into Eq. [12]-[14] yields the following dimensionless initial and boundary conditions

$$\text{at } t = 0 \quad \Theta_1(\xi, t) = \Theta_1(\xi, 0) = \frac{c_1^*(x)}{c_F} = \psi_1(\xi) \quad [20]$$

$$\text{for } t > 0 \text{ at } \xi = 0 \quad \Theta_1(\xi, t) = \Theta_1(0, t) = \frac{E}{c_F} = EP \quad [21]$$

$$\text{for } t > 0 \text{ at } \xi = 1 \quad \left.\frac{\partial \Theta_1}{\partial \xi}\right|_{\xi=1} = -H[\Theta_1(1, t) - B] \quad [22]$$

where

$$H = \frac{\mathbf{F} i N_M L}{RT\kappa} \quad [23]$$

and

$$B = \frac{RT\kappa}{\mathbf{F}^2 D_1 c_F} \quad [24]$$

As shown in Eq. [20], $c_1^*(x)$ or $\psi_1(\xi)$ corresponds to a steady-state solution of the simple steady-state model, which is a result of a previously set current density (i^*) and head (h^*). Thus, $c_1^*(x)$ is a known quantity that depends only on position within the diaphragm and not on time. This concentration distribution results from the solution of the steady-state material balance equation (3, 4)

$$\frac{d^2 c_1^*}{d\xi^2} - A_1^* \frac{dc_1^*}{d\xi} = 0 \quad [25]$$

where

$$A_1^* = \frac{-\mathbf{F} i^* N_M L}{RT\kappa} + \frac{\rho g h^* PN_M}{\mu D_1} \quad [26]$$

subject to the boundary conditions

$$\text{at } \xi = 0 \qquad c_1^*(0) = E \quad [27]$$

and

$$\text{at } \xi = 1 \qquad \left.\frac{dc_1^*}{d\xi}\right|_{\xi=1} = \frac{-\mathbf{F} i^* N_M L}{RT\kappa} c_1^*(L) + \frac{i^* N_M L}{D_1 \mathbf{F}} \quad [28]$$

Integration of Eq. [25] with Eq. [27] and [28] yields an expression for c_1^* and the dimensionless OH^- concentration $\psi_1(\xi)$ at $t = 0$

$$\psi_1(\xi) = \frac{E}{c_F} + G_1 [\exp(A_1^* \xi) - 1] \quad [29]$$

where

$$G_1 = \frac{\dfrac{i^* N_M L}{D_1 \mathbf{F} c_F} - \dfrac{\mathbf{F} i^* N_M L E}{RT\kappa c_F}}{\dfrac{\rho g h^* PN_M}{\mu D_1} \exp(A_1^*) - \dfrac{\mathbf{F} i^* N_M L}{RT\kappa}} \quad [30]$$

The governing partial differential equation for $\Theta_1(\xi, t)$, Eq. [17], can be integrated analytically subject to Eq. [20]-[22] by using the transformation suggested by Bastian and Lapidus (27, 28) as shown in the Appendix. The resulting expression for the dimensionless concentration of OH^- ion in the diaphragm can be written as follows

$$\Theta_1(\xi, t) = EP + G_2[\exp(A_1 \xi) - 1] + \exp\left[\frac{A_1 \xi}{2} - \frac{A_1^2 t}{4\gamma}\right] \left\{\sum_{N=0}^{\infty} \mathbf{F}_N \sin(\lambda_N \xi) \exp\left(\frac{-\lambda_N^2 t}{\gamma}\right)\right\} \quad [31]$$

where

$$G_2 = \frac{HB - HEP}{\dfrac{\rho g h PN_M}{\mu D_1} \exp(A_1) - H} \quad [32]$$

and

$$\mathbf{F}_N = \frac{4\lambda_N}{(2\lambda_N - \sin 2\lambda_N)} \left[\frac{G_1 \left\{\lambda_N + \left[\left(A_1^* - \frac{A_1}{2}\right) \sin \lambda_N - \lambda_N \cos \lambda_N\right] \exp\left(A_1^* - \frac{A_1}{2}\right)\right\}}{\left(A_1^* - \frac{A_1}{2}\right)^2 + \lambda_N^2} + \frac{(G_2 - G_1) \left\{\lambda_N - \left[\frac{A_1}{2} \sin \lambda_N + \lambda_N \cos \lambda_N\right] \exp\left(-\frac{A_1}{2}\right)\right\}}{\frac{A_1^2}{4} + \lambda_N^2} - \frac{G_2 \left\{\lambda_N + \left[\frac{A_1}{2} \sin \lambda_N - \lambda_N \cos \lambda_N\right] \exp\left(\frac{A_1}{2}\right)\right\}}{\frac{A_1^2}{4} + \lambda_N^2} \right] \quad [33]$$

and where the eigenvalues, λ_N, are the roots of

$$\lambda_N \cot \lambda_N + \left(H + \frac{A_1}{2}\right) = 0 \quad [34]$$

Next, consider the unsteady-state material balance for the OH^- ions in the catholyte, which, with assumptions (*viii*)-(*x*), can be written as follows

$$\frac{dc_{1,\text{eff}}}{dt} = \frac{vA_d}{V_c} c_1(L, t) - \frac{vA_d}{V_c} c_{1,\text{eff}} \quad [35]$$

where v is given by Eq. [7] and V_c is the volume of the catholyte. Recall that, according to assumption (ix), the catholyte is a completely mixed flow reactor, which means that the effluent concentration $c_{1,\text{eff}}$ is the same as the catholyte concentration, and the inlet concentration to the catholyte compartment, $c_1(L, t)$, is typically different from $c_{1,\text{eff}}$ during transients. An appropriate initial condition for the catholyte concentration is its value at steady state before a transient

$$\text{at } t = 0 \qquad c_{1,\text{eff}} = c_1^*(L) \quad [36]$$

Equation [35] can be integrated analytically by using Eq. [31] to obtain an expression for $c_1(L, t)$ (*i.e.*, $c_F\,\Theta(1, t)$). That is

$$c_{1,\text{eff}}\left[\exp\left(\frac{vA_d t}{V_c}\right)\right] = \frac{vA_d}{V_c}\int c_F\,\Theta_1(1, t)\exp\left(\frac{vA_d t}{V_c}\right) dt + G_{10} \quad [37]$$

where G_{10} is an integration constant. Evaluation of G_{10} by using Eq. [36] yields

$$c_{1,\text{eff}} = c_F\left\{EP + G_2\left[\exp(A_1) - 1\right]\right\}\left[1 - \exp\left(\frac{-vA_d t}{V_c}\right)\right] + c_F \exp\left[\frac{A_1}{2} - \frac{A_1^2 t}{4\gamma}\right]\left\{\sum_{N=0}^{\infty} G_{11}F_N \sin(\lambda_N)\exp\left(\frac{-\lambda_N^2 t}{\gamma}\right)\right\} - c_F \exp\left[\frac{A_1}{2} - \frac{vA_d t}{V_c}\right]\left\{\sum_{N=0}^{\infty} G_{11}F_N \sin\lambda_n\right\} + c_1^*(L)\exp\left(\frac{-vA_d t}{V_c}\right) \quad [38]$$

where

$$G_{11} = \frac{\dfrac{vA_d}{V_c}}{\dfrac{vA_d}{V_c} - \dfrac{A_1^2}{4\gamma} - \dfrac{\lambda_N^2}{\gamma}} \quad [39]$$

Equation [38] can be used to obtain an expression for the time-dependent caustic yield, $\eta(t)$, (often referred to as the caustic current efficiency) by using the following definition

$$\eta(t) = \frac{P\rho hgFc_{1,\text{eff}}}{\mu Li} \quad [40]$$

Discussion

The model presented above can be used to investigate the dynamic behavior of a diaphragm cell in terms of step changes in either the current density or the differential head (not discussed here). The model also allows consideration of two distinct initial conditions; that is, the behavior of the cell can be analyzed during start-up, where the initial concentration is a constant for all ξ, or during a change from one steady state to another, where the initial concentration is a function of ξ. Figures 2-4 show the predictions of the model for the two different initial conditions when the parameters of Table I are used. Figure 2 shows the concentration profiles in the diaphragm during start-up for an initial concentration of OH^- of $10^{-7}M$ (corresponding to no current) and a step change in current density from 0 to 0.1543 A/cm^2 at $t = 0$. Figure 3 presents the concentration profiles in the diaphragm for a step change in current density from 0.054 to 0.1543 A/cm^2 at $t = 0$. In both Fig. 2 and 3, the final steady state is

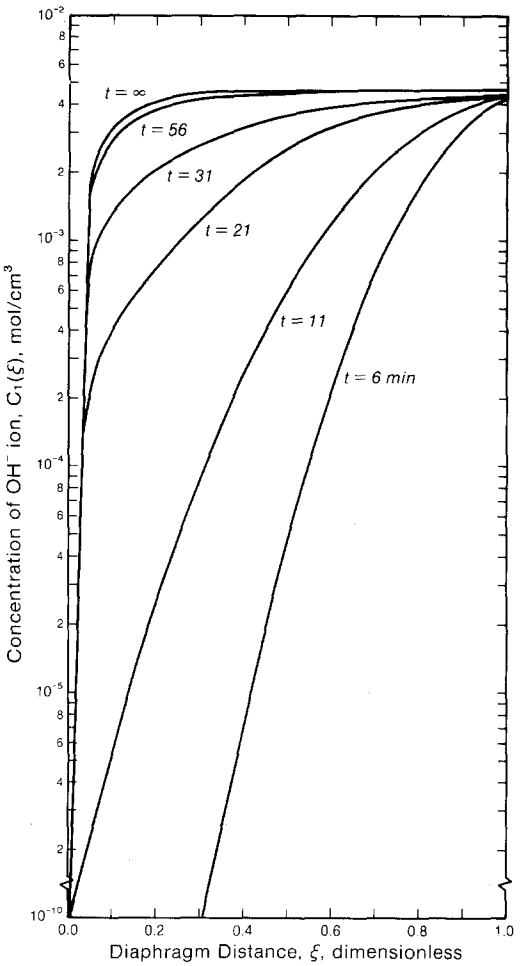

Fig. 2. Concentration profiles during start-up (*i.e.*, a step in the current density from $i^* = 0$ to $i = 0.1543$ A/cm^2).

achieved approximately after 56 min. This rather quick response illustrates that the response time of the diaphragm is not on the order of γ (*i.e.*, 8h for Table I values), as would be expected in a system governed solely by diffusion, but instead is faster because of the convection-like term

$$\left(A_1 \frac{\partial\Theta_1}{\partial\xi}\right)$$

in Eq. [17]. On the other hand, Fig. 4 shows that the time-dependent responses of the cell effluent concentration for the cases shown in Fig. 2 and 3 are on the order of 10h (*i.e.*, $\approx$ 63% of the final steady-state value), as would be expected from Eq. [35], since $V_c/(vA_d)$ is on the order of 9h.

Table I. Parameters for calculations shown in Fig. 2-5

Physical Constants		
	c_F	$= 5.00 \times 10^{-3}$ mol/cm^3
	D_1	$= 3.50 \times 10^{-5}$ cm^2/s
	E	$= 1.00 \times 10^{-10}$ mol/cm^3
	κ	$= 0.50\ \Omega^{-1}$ cm^{-1}
	μ	$= 1.10 \times 10^{-2}$ g/cm-s
	ρ	$= 1.17$ g/cm^3
Cell Geometry		
	A_d/V_c	$= 0.20$ cm^{-1}
Diaphragm Properties		
	N_M	$= 2.00$
	P	$= 5.80 \times 10^{-11}$ cm^2
	L	$= 1.00$ cm
	ϵ	$= 0.50$
Operating Variables		
	h^*	= 25.0 cm, except Fig. 5
	h	= 25.0 cm, except Fig. 5
	i^*	= see figure captions and text
	i	= see figure captions and text
	T	= 358.15 K

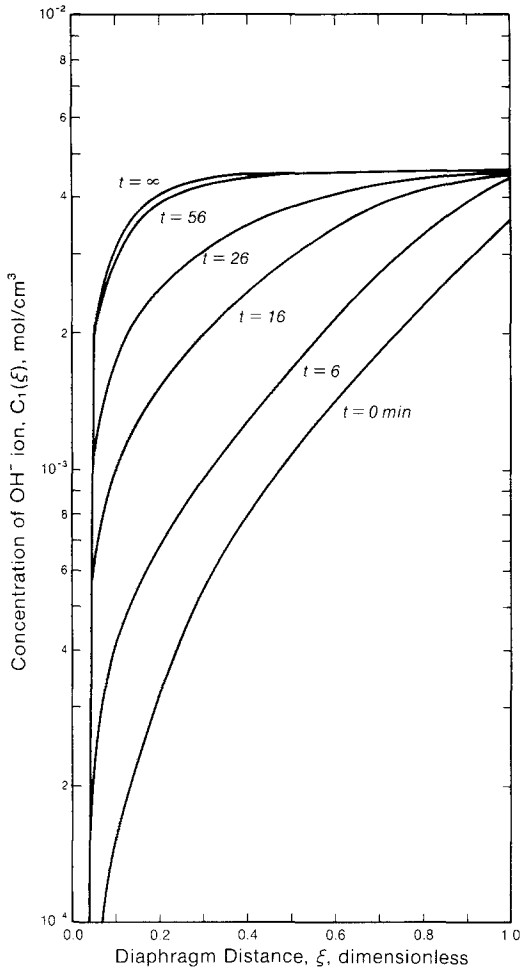

Fig. 3. Concentration profiles for a step change in current density from $i^* = 0.0540$ A/cm² to $i = 0.1543$ A/cm².

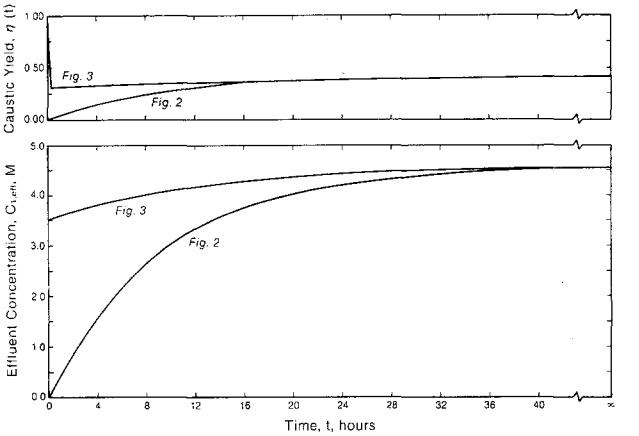

Fig. 4. Effluent concentration and caustic yield profiles corresponding to Fig. 2 and 3.

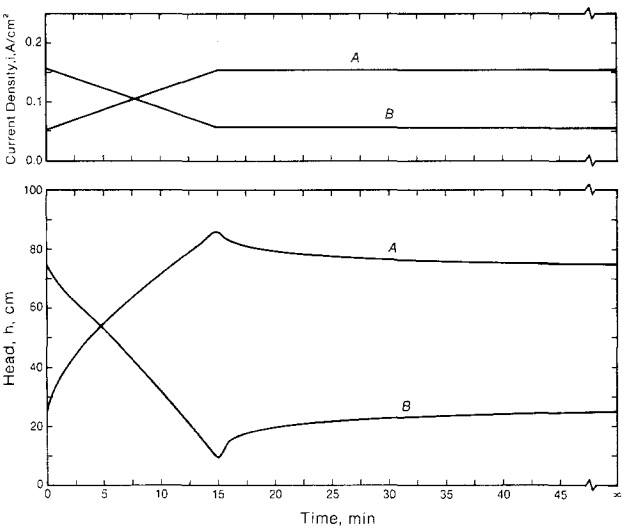

Fig. 5. Relationship between current density and head required to maintain a constant caustic effluent concentration of 3.541×10^{-3} mol/cm³.

Instead of determining the response of the cell to a step change in (i), it may be more desirable to maintain the effluent concentration at a previous steady-state value[2] and simply increase or decrease the production rate by adjusting the head and current densities simultaneously. This change in the production rate might be desirable if, for example, a differential cost structure for electricity provided an incentive for a high production rate at night and a low production rate during the day. In such a case, a constant effluent concentration may simplify the operation of evaporators that are connected in series to the electrolyzers.

Unfortunately, the analytical solution presented above cannot be used to predict the time-dependent head required to maintain a constant effluent concentration because A_1 is a function of time in this case. However, Eq. [17] can be integrated numerically. To do this, implicit stepping accurate to $0(\Delta t)$ was used with a finite difference technique accurate to $0((\Delta\xi)^2)$ (29-31) in a manner similar to that in Ref. (32, 33) and then with a finite difference technique accurate to $0((\Delta\xi)^4)$ (34) to first verify the profiles of Fig. 2 and 3 and then to produce (16) Fig. 5.[3] Curve A in Fig. 5 shows how to change the head with time so that $c_{1,eff}$ remains constant at 3.54×10^{-3} mol/cm³ when the current density is increased linearly from 0.054 to 0.1543 A/cm² in 15 min. Similarly, curve B shows how to decrease the head as the current density is decreased linearly from 0.1543 to 0.054 A/cm² so that $c_{1,eff}$ remains constant at 3.54×10^{-3} mol/cm³. For the results shown in Fig. 5, the caustic yield, $\eta(t)$, changes from about 0.96 to 0.99 for curve A and then from 0.99 to 0.96 for curve B while the molar production rate of NaOH ($vc_{1,eff}$ with v given by Eq. [7]) is increased and then decreased by a factor of three in curves A and B, respectively; that is, h changes from 25 cm at $t = 0$ to 75 cm at $t = \infty$ for curve A and from 75 cm at $t = 0$ to 25 cm at $t = \infty$ for curve B.

[2]The criterion for an effluent concentration that is constant with respect to time is that the concentration at the diaphragm/catholyte interface be constant with respect to time (see Eq. [35] and [36]).

[3]Figure 5 was prepared by inputing the current density at a particular time and then iterating h (using reguli-falsi) until $c_1(1, t) = 3.54 \times 10^{-3}$ mol/cm³ according to the numerical integration of Eq. [11].

Conclusions

The development of a simple time-dependent model for OH^- ion in the diaphragm and the catholyte in terms of measurable diaphragm properties and cell geometry provides a design equation that could be used for future comparison of experimental data and theoretical predictions. A numerical solution of the model equations provides a method that could be used in a control scheme to maintain a constant hydroxyl ion concentration in the effluent, subject to an arbitrary change of the current density.

Acknowledgment

The authors acknowledge gratefully that this work was supported in part by Dow Chemical USA.

Manuscript submitted July 6, 1984; revised manuscript received Nov. 8, 1985.

APPENDIX

The governing partial differential equation for OH^- in the diaphragm is

$$\gamma \frac{\partial \Theta_1}{\partial t} = \frac{\partial^2 \Theta_1}{\partial \xi^2} - A_1 \frac{\partial \Theta_1}{\partial \xi} \qquad [A\text{-}1]$$

and the initial and boundary conditions are

$$at\ t = 0 \qquad \Theta_1(\xi, 0) = \psi_1(\xi) \qquad [A\text{-}2]$$

$$for\ t > 0\ at\ \xi = 0 \qquad \Theta_1(0, t) = EP \qquad [A\text{-}3]$$

for $t > 0$ at $\xi = 1$ $$\left.\frac{\partial \Theta_1}{\partial \xi}\right|_{\xi=1} = -H[\Theta_1(1, t) - B] \quad [A\text{-}4]$$

where H and B are given respectively by Eq. [23] and [24] in the text.

The solution to these equations can be obtained by assuming a solution of the form

$$\Theta_1(\xi, t) = Y_1(\xi, t) + \Gamma_1(\xi) \quad [A\text{-}5]$$

Substitution of Eq. [A-5] into Eq. [A-1] gives an expression that can be divided arbitrarily into two equations

$$\frac{d^2\Gamma_1}{d\xi^2} - A_1 \frac{d\Gamma_1}{d\xi} = 0 \quad [A\text{-}6]$$

$$\gamma \frac{\partial Y_1}{\partial t} = \frac{\partial^2 Y_1}{\partial \xi^2} - A_1 \frac{\partial Y_1}{\partial \xi} \quad [A\text{-}7]$$

Similarly, the initial conditions and boundary conditions are separable and can be written

at $t = 0$ $$Y_1(\xi, 0) = \psi_1(\xi) - \Gamma_1(\xi) \quad [A\text{-}8]$$

for $t > 0$ at $\xi = 0$ $$Y_1(0, t) = 0 \quad [A\text{-}9]$$

$$\Gamma_1(0) = EP \quad [A\text{-}10]$$

for $t > 0$ at $\xi = 1$ $$\left.\frac{\partial Y_1}{\partial \xi}\right|_{\xi=1} = -HY_1(1, t) \quad [A\text{-}11]$$

$$\left.\frac{d\Gamma_1}{d\xi}\right|_{\xi=1} = -H[\Gamma_1(1) - B] \quad [A\text{-}12]$$

Integration of Eq. [A-6] twice yields

$$\Gamma_1(\xi) = V_1 + V_2 \exp(A_1\xi) \quad [A\text{-}13]$$

where V_1 and V_2 are constants of integration that can be obtained from application of Eq. [A-10] and [A-12] to Eq. [A-13], which yields

$$\Gamma_1(\xi) = EP + G_2[\exp(A_1\xi) - 1] \quad [A\text{-}14]$$

where G_2 is defined by Eq. [32] in the text.

Equation [A-7] can be integrated by using the transformation suggested by Bastain and Lapidus (27, 28); that is, let

$$Y_1(\xi, t) = w_1(\xi, t) \exp\left[\frac{A_1\xi}{2} - \frac{A_1^2 t}{4\gamma}\right] \quad [A\text{-}15]$$

so that Eq. [A-7] becomes

$$\gamma \frac{\partial w_1}{\partial t} = \frac{\partial^2 w_1}{\partial \xi^2} \quad [A\text{-}16]$$

and the initial and boundary conditions become

at $t = 0$ $$w_1(\xi, 0) = [\psi_1(\xi) - \Gamma_1(\xi)] \exp\left(\frac{-A_1\xi}{2}\right) \quad [A\text{-}17]$$

for $t > 0$ at $\xi = 0$ $$w_1(0, t) = 0 \quad [A\text{-}18]$$

for $t > 0$ at $\xi = 1$ $$\left.\frac{\partial w_1}{\partial \xi}\right|_{\xi=1} = -\left(H + \frac{A_1}{2}\right) w_1(1, t) \quad [A\text{-}19]$$

Equation [A-16] can be integrated with the method of separation of variables by assuming that

$$w_1(\xi, t) = U(\xi)\, Z(t) \quad [A\text{-}20]$$

Substitution of Eq. [A-20] into Eq. [A-16] yields

$$\frac{\gamma}{Z}\frac{dZ}{dt} = \frac{1}{U}\frac{d^2U}{d\xi^2} = -\lambda_N^2 \quad [A\text{-}21]$$

and the boundary conditions become

for $t > 0$ at $\xi = 0$ $$U(0) = 0 \quad \text{for all } Z(t) \quad [A\text{-}22]$$

for $t > 0$ at $\xi = 1$ $$\left|\frac{dU}{d\xi}\right|_{\xi=1} = -\left(H + \frac{A_1}{2}\right) U(1) \quad \text{for all } Z(t) \quad [A\text{-}23]$$

Thus $Z(t)$ and $U(\xi)$ have the general forms

$$Z(t) = G_3 \exp\left(\frac{-\lambda_N^2 t}{\gamma}\right) \quad [A\text{-}24]$$

and

$$U(\xi) = G_4 \sin(\lambda_N\xi) + G_5 \cos(\lambda_N\xi) \quad [A\text{-}25]$$

where G_3, G_4, and G_5 are integration constants.

Application of the boundary condition [A-22] to Eq. [A-25] yields

$$G_5 = 0 \quad [A\text{-}26]$$

and application of Eq. [A-23] to Eq. [A-25] yields the eigenvalues, which are roots of the following equation

$$\lambda_N \cot \lambda_N + \left(H + \frac{A_1}{2}\right) = 0 \quad [A\text{-}27]$$

Thus the complete general solution for $w_1(\xi, t)$ is

$$w_1(\xi, t) = \sum_{N=0}^{\infty} \mathbf{F}_N \sin(\lambda_N\xi) \exp\left(\frac{-\lambda_N^2 t}{\gamma}\right) \quad [A\text{-}28]$$

The constants $\mathbf{F}_N$ in Eq. [A-28] can be evaluated using the initial condition and the principle of orthogonality. That is, at $t = 0$

$$\sum_{N=0}^{\infty} \mathbf{F}_N \sin(\lambda_N\xi) = [\psi_1(\xi) - \Gamma_1(\xi)] \exp\left(\frac{-A_1\xi}{2}\right) \quad [A\text{-}29]$$

Multiplying both sides of Eq. [A-29] by $\sin(\lambda_M\xi)$ and integrating yields

$$\sum_{N=0}^{\infty} \mathbf{F}_N \int_0^1 \sin(\lambda_N\xi) \sin(\lambda_M\xi) d\xi = \int_0^1 [\psi_1(\xi) - \Gamma_1(\xi)] \exp\left(\frac{-A_1\xi}{2}\right) \sin(\lambda_M\xi) d\xi \quad [A\text{-}30]$$

The left-hand side of Eq. [A-30] is zero for $N \neq M$; thus

$$\mathbf{F}_N = \frac{4\lambda_N}{(2\lambda_N - \sin 2\lambda_N)} \int_0^1 [\psi_1(\xi) - \Gamma_1(\xi)] \exp\left(\frac{-A_1\xi}{2}\right) \sin(\lambda_N\xi) d\xi \quad [A\text{-}31]$$

which after integration yields the expression given by Eq. [33] in the text.

Finally, the complete solution for $\Theta_1(\xi, t)$ can be written by using Eq. [A-5], [A-14], [A-15], and [A-28]

$$\Theta_1(\xi, t) = EP + G_2[\exp(A_1\xi) - 1] + \exp\left[\frac{A_1\xi}{2} - \frac{A_1^2 t}{4\gamma}\right] \left\{\sum_{N=0}^{\infty} \mathbf{F}_N \sin(\lambda_N\xi) \exp\left(\frac{-\lambda_N^2 t}{\gamma}\right)\right\} \quad [A\text{-}32]$$

LIST OF SYMBOLS

A_d	area of the diaphragm, cm^2
A_1, A_1*	dimensionless driving force at $t > 0$ and $t = 0$, respectively, see Eq. [19] and [26]
B	see Eq. [24], dimensionless
c_i	concentration of species i, mol/cm^3
c_1, $c_1(x, t)$	concentration of OH^- ion at $t > 0$, mol/cm^3
c_1*, c_1*(x)	concentration of OH^- ion at $t = 0$, mol/cm^3
$c_{1,\text{eff}}$	effluent NaOH concentration, mol/cm^3
$c_{\mathbf{F}}$	NaCl feed concentration, a constant reference quantity, mol/cm^3
D_i	free-stream diffusion coefficient of species i, cm^2/s
D_1	free-stream diffusion coefficient of OH^- ion, cm^2/s
D_a	axial dispersion coefficient in porous region, cm^2/s

$D_{i,e}$	effective diffusion coefficient of species i, cm²/s
$D_{i,o}$	free-stream diffusion coefficient divided by tortuosity, cm²/s
E	equilibrium concentration of OH^- ion at anolyte/diaphragm interface (*e.g.*, 10^{-10} mol/cm³ at 298 K)
EP	dimensionless equilibrium concentration, see Eq. [21]
$\mathbf{F}$	Faraday's constant, 96,487 C/mol of electrons
$\mathbf{F}_N$	see Eq. [33], dimensionless
G_1	see Eq. [30], dimensionless
G_2	see Eq. [32], dimensionless
G_3, G_4, G_5	integration constants, dimensionless
G_{10}	integration constant, mol/cm³
G_{11}	see Eq. [39], dimensionless
g	acceleration due to gravity, cm/s²
H	dimensionless potential gradient, see Eq. [23]
h, h^*	differential head at $t > 0$ and $t = 0$, respectively, cm
i, i^*	current density at $t > 0$ and $t = 0$, respectively, A/cm²
L	diaphragm thickness, cm
M, N	summation indexes
N_M	MacMullin number, see Eq. [2], dimensionless
$\underline{N}_i$, N_i	flux of species i, mol/cm²-s
P	Darcy's law permeability, cm²
R	gas constant, 8.3143 J/mol-K
T	temperature of the cell, K
t	time, s
u_i	ionic mobility of species i, cm²-mol/J-s
V_c	volume of catholyte, cm³
$\underline{v}$	superficial velocity vector, cm/s
$\underline{V}$	superficial velocity through the diaphragm, cm/s
x	diaphragm dimensional coordinate, cm
z_i	ionic charge of species i, $z_i = -1$, dimensionless

Greek

$\underline{\nabla}$	divergence vector, cm⁻¹
ϵ	porosity, dimensionless
η, $\eta(t)$	caustic yield or caustic current efficiency, see Eq. [40], dimensionless
γ	diaphragm time constant, see Eq. [18], s⁻¹
κ	average solution conductivity, Ω^{-1} cm⁻¹
λ_N	eigenvalues see Eq. [34], dimensionless
μ	average solution viscosity, g/cm-s
Φ, $\Delta\Phi$	dimensional voltage, voltage drop through the diaphragm, V
$\psi_i(\xi)$	dimensionless concentration at $t = 0$ see Eq. [29]
ρ	anolyte solution density, g/cm³
ρ_*	resistivity of diaphragm filled with electrolyte, Ω-cm
ρ_o	resistivity of the electrolyte, Ω-cm
τ	tortuosity of diaphragm, dimensionless
Θ_i, $\Theta_i(\xi, t)$	dimensionless concentration of OH^- ion at position ξ and time t
ξ	dimensionless coordinate, see Eq. [15]

REFERENCES

1. W. B. Darlington and M. Y. C. Woo, *This Journal*, **129**, 275C (1982).
2. K. A. Poush, D. L. Caldwell, J. W. Van Zee, and R. E. White, in "Modern Chlor-Alkali Technology," Vol. 2, C. Jackson, Editor, pp. 21-33, Ellis Horwood Limited, Chichester, West Sussex, England (1983).
3. R. E. White, J. S. Beckerdite, and J. Van Zee, in "Electrochemical Cell Design," R. E. White, Editor, pp. 25-60, Plenum Press, New York (1984).
4. J. Van Zee and R. E. White, *This Journal*, **132**, 818 (1985).
5. D. L. Caldwell, K. A. Poush, J. W. Van Zee, and R. E. White, in "Electrochemical Processes and Plant Design," R. C. Alkire, T. R. Beck, and R. D. Varjian, Editors, p. 216, The Electrochemical Society Softbound Proceedings Series, Pennington, NJ (1983).
6. R. B. MacMullin and G. A. Muccini, *J. AIChE*, **2**, 393 (1956).
7. F. Hine, M. Yasuda, and K. Fujita, *This Journal*, **128**, 2314 (1981).
8. L. G. Austin, "Handbook of Fuel Cell Technology," p. 160, Prentice-Hall Inc., Englewood Cliffs, NJ (1968).
9. V. V. Stender, O. S. Ksenzhek, and V. N. Lazarev, *Zh. Prik. Khim.*, **40**, 1293 (1967).
10. W-H. Koh, *AIChE Symposium Series*, **77**, 213 (1981).
11. T. Mukaibo, *J. Electrochem. Soc. Jpn.*, **20**, 482 (1952).
12. F. Hine, M. Yasuda, and T. Tanka, *Electrochim. Acta*, **22**, 429 (1977).
13. F. Hine, *Soda to enso*, 219-233, June 1980.
14. R. R. Chandran, D. T. Chin, and K. Viswanathan, *J. Appl. Electrochem.*, **14**, 511 (1984).
15. V. L. Kubasov, V. B. Vorbena, and L. I. Yurkov, *Sov. Electrochem.*, **15**, 1773 (1979).
16. J. W. Van Zee, Ph.D. Dissertation, Texas A&M University, College Station, TX (1984).
17. M. Schleiff, G. Lefeld, and H. Matschiner, *Chem. Tech., (Leipzig)*, **35**, 193 (1983).
18. V. P. Filatov and V. N. Golubetskii, *J. App. Chem. USSR*, **52**, 2160 (1979).
19. V. P. Filatov and G. V. Tsibizov, *ibid.*, **52**, 2157 (1979).
20. V. P. Filatov and G. V. Tsibizov, *ibid.*, **52**, 2153 (1979).
21. V. P. Filatov, A. L. Rotinyan, and G. V. Tsibizov, *ibid.*, **49**, 1571 (1976).
22. F. M. Kummerle and P. R. Roberge, Abstract 409, p. 672, The Electrochemical Society Extended Abstracts, Vol. 82-1, Montreal, Quebec, Canada (May 9-14, 1982).
23. J. S. Dunning, Ph.D. Dissertation, University of California, Los Angeles (1971).
24. J. Newman and W. Tiedemann, *AIChE J.*, **21**, 25 (1975).
25. J. A. Trainham, Ph.D. Dissertation, University of California, Berkeley (1979).
26. J. S. Newman, "Electrochemical Systems," Prentice-Hall, Inc., Englewood Cliffs, NJ (1973).
27. W. C. Bastain and L. Lapidus, *J. Phys. Chem.*, **60**, 816 (1956).
28. J. H. Seinfeld and L. Lapidus, "Mathematical Methods in Chemical Engineering; Volume 3, Process Modeling, Estimation and Identification," p. 129, Prentice-Hall, Inc., Englewood Cliffs, NJ (1974).
29. J. S. Newman, "Electrochemical Systems," Appendix C, Prentice-Hall, Inc., Englewood Cliffs, NJ (1973).
30. J. S. Newman, *Ind. Eng. Chem. Fundam.*, **7**, 514 (1968).
31. R. E. White, *ibid.*, **17**, 367 (1978).
32. W. H. Tiedemann and J. Newman, in "Battery Design and Optimization," S. Gross, Editor, p. 25, The Electrochemical Society Softbound Proceedings Series, Princeton, NJ (1979).
33. R. E. White, M. Bain, and M. Raible, *This Journal*, **131**, 855 (1982).
34. J. Van Zee, L. G. Kliene, R. E. White, and J. Newman, in "Electrochemical Cell Design," R. E. White, Editor, pp. 377-389, Plenum Press, New York (1984).